# POLARIZATION OBSERVABLES AND HADRON STRUCTURE: EXPERIMENT AND THEORY.

Egle Tomasi-Gustafsson*
DAPNIA/SPhN, CEA/Saclay, 91191 Gif-sur-Yvette Cedex, France

**Abstract**

Selected problems relative to the study of the electromagnetic structure of hadrons are presented. Elastic electromagnetic form factors of proton, neutrons and deuterons are discussed: the methods used for the measurements, the available results and their interpretation. Special attention is devoted to a general description in all the kinematical region, including asymptotic properties.

## 1 Introduction

The electromagnetic structure of hadrons represents a traditional field of research in nuclear and particle physics in the intermediate energy region. Such region is defined by beam energies of a few GeV, corresponding to a wavelength smaller than 1 fm, the dimension of the nucleon. Lepton probes as electron or muons, being structureless, are in general preferred to hadronic probes, although, as it will be discussed later, radiative corrections can induce large complexity in the analysis and in the interpretation of the results. The traditional way to measure hadron electromagnetic FFs is based on elastic scattering of electrons. In the intermediate region of momentum transfer squared one of the the main physical issues, related to the study of the deuteron structure, is to determine the kinematical region where the transition to pQCD occurs, i.e. where a description in terms

*E-mail:Egle.Tomasi@cea.fr

of quark and gluon degrees of freedom would be more adequate than a picture based on mesons effective theories.

Recently, precise measurements of elastic scattering of electrons on nucleons, deuteron and light nuclei have been made possible by the construction of 100% duty cycle electron accelerators, high resolution spectrometers, highly polarized beams and polarimeters which can measure the proton, neutron and deuteron polarization in the GeV range.

In a P and T invariant theory, the electromagnetic structure of a hadron with spin $S$ is described by $2S+1$ form factors (FFs). The nucleon has two elastic FFs, electric, $G_E$, and magnetic, $G_M$, or alternatively the Pauli and Dirac FFs, $F_1$ and $F_2$, which are a linear combination of the previous ones. They seem more fundamental, as they enter into a parametrization of the electromagnetic current in a relativistic and gauge-invariant form, valid in any coordinate system. The deuteron, which is an isoscalar, spin one particle, is described by three FFs, charge, magnetic and quadrupole. FFs are real functions of one kinematical variabe only, $Q^2$, in the space-like (SL) (scattering) region, if one assumes that the interaction takes place through the exchange of a virtual photon, of four–momentum $Q^2$. They are complex functions in time-like region (TL), which is explored in annihilation reactions of two leptons into two hadrons and in the time-reverse reaction.

In this series of lectures we will give a view on the present understanding of the electromagnetic structure of hadrons. The methods of measurement are presented, the present data illustrated and the open issues underlined.

# 2 Experimental methods

The expression of the unpolarized cross section for electron elastic scattering on any hadron, is expressed in all cases through two structure functions, real functions of $Q^2$ only. This derives from the assumption that the interaction takes place through the exchange of a virtual photon, of four–momentum $Q^2$. In case of proton, one defines a *reduced* cross section, function of the FFs which contain the dynamics of the reaction, after factorizing some kinematical terms:

$$\sigma_{red} = \epsilon(1+\tau)\left[1+2\frac{E}{m}\sin^2(\theta/2)\right]\frac{4E^2\sin^4(\theta/2)}{\alpha^2\cos^2(\theta/2)}\frac{d\sigma}{d\Omega} = \tau G_{Mp}^2 + \epsilon G_{Ep}^2, \quad (1)$$

$$\epsilon = [1+2(1+\tau)\tan^2(\theta/2)]^{-1},$$

where $\alpha = 1/137$, $\tau = Q^2/(4m^2)$, $Q^2$ is the momentum transfer squared, $m$ is the proton mass, $E$ and $\theta$ are the incident electron energy and the scattering angle of the outgoing electron, respectively, and $G_{Mp}$ and $G_{Ep}$ are the magnetic and the electric proton FFs.

Measurements of the elastic differential cross section at different angles for a fixed value of $Q^2 = -4EE_f \sin^2(\theta/2)$ ($E_f$ is the scattered electron energy) allow $G_{Ep}$ and $G_{Mp}$ to be determined as the slope and the intercept, respectively, from the linear $\epsilon$ dependence (1). For each $Q^2$ point, one has to change incident energy and scattering angle. In TL region, Ffs are extracted from the angular distribution of the final particle, at a fixed value of the total energy $s$.

In case of deuteron, a third observable is necessary, in order to make the full separation of the three FFs, in general the tensor polarization of the scattered deuteron, in the unpolarized *ed* elastic scattering, $t_{20}$.

In any case, the unpolarized cross section contains the FFs squared, and does not allow to determine their sign. This method, called the Rosenbluth separation [1], is very efficient at low $Q^2$, but already in 1967 A.I. Akhiezer and M.P. Rekalo proved that the measurement of the polarization of the scattered proton, in the elastic scattering of longitudinally polarized protons, contains a more precise information on the FFs, as it depends by an interference term, which is proportional to the product $G_E G_M$ and concluded that '*Thus, there exist a number of polarization experiments which are more effective for determining the proton charge form factor than is the measurement of the differential cross section for unpolarized particles*' [2].

The GEP collaboration at JLab showed that very precise data on the ratio $G_{Ep}/G_{Mp}$ can be obtained by measuring the ratio of the longitudinal to transverse polarization $P_L/P_T$ [3]. For this aim, it is necessary to have a high intensity, high polarized and stable electron beam, high precision spectrometers and especially polarimeters: specific detectors which can measure the proton polarization polarization in the GeV range.

## 2.1 Hadron polarimeters

The working principle of hadron polarimeters is the measurement of the azimuthal asymmetry in a secondary scattering on a light target, hydrogen or carbone, for example. This can be obtained with the help of a set up which measures the trajectory of the polarized particle in the focal plane

of a spectrometer, a second thick target, and a detection downstream, which detects the products of the secondary scattering. The secondary reaction must have large cross section and large analyzing powers, in order to reduce statistical and systematic errors. For measuring proton and deuteron (vector) polarization, it has been shown that a semi-inclusive reaction as $p+C \rightarrow one\ charged\ particle+X$ is sufficient (although in case of deuteron one must eliminate deuteron break up). For tensor polarization of the deuteron, an exclusive reaction such as $dp$ elastic scattering or $dp \rightarrow ppn$ charge exchange have very large analyzing power. The first reaction was used in a polarimeter HYPOM [4] to study the $^3He$ structure [5], the second one was used in the POLDER [6] polarimeter, to measure the $t_{20}$ polarization in unpolarized $ed$ scattering and the deuteron form factors at JLab [7]. The fact that this reaction has very large tensor analyzing powers was firstly suggested by I. Pomeranchuk [8] and can be understood because the deuteron has spin $S = 1$, isopin $I = 0$. If one select a pair of protons in final $S = 0$ state, the Pauli principle requires a spin-flip, and the corresponding amplitude contributes to large tensor analyzing power. The performance of a polarimeter is expressed in terms of the figure of merit

$$\mathcal{F} = \int_\theta \epsilon(\theta) A^2(\theta) d\theta \tag{2}$$

where the integration is done over the angular range of the detection, $\epsilon$ is the efficiency, i.e. the number of useful events emitted at an angle $\theta$ normalized to the number of incident particles $N_{inc}$, and $A$ is the analyzing power. This quantity is especially useful, because it allows to estimate the number of events in order to obtain a given uncertainty in a polarization measurement, $\Delta P = \sqrt{2} N_{inc} \mathcal{F}^2$.

One can see that the large analyzing powers are essential for a measurement. We can summarize the main aspects of polarimetry:

- precise determination of ingoing and ougoing trajectories, to avoid systematic errors which would give instrumental azymuthal asymmetries

- search for the best analyzing reaction, depending on the polarized particle momentum;

- improvement of the figure of merit by adjusting the thickness and the geometry of the target [9].

# 3 Results and Consequences

## 3.1 Space-like and time-like regions

Let us summarize a few aspects of the experimental data, which are presently available. The $Q^2$-behavior of nucleon electromagnetic FFs is consistent with:

- "standard" dipole function for the nucleon magnetic FFs $G_{Mp}$ and $G_{Mn}$,
- linear deviation from the dipole function for the electric proton FF $G_{Ep}$,
- non vanishing electric neutron FF, $G_{En}$.

In time-like region:

- No separation has been done between $G_E$ and $G_M$.
- $G_M$, extracted under the hypothesis $G_E = G_M$ (valid only at threshold) show a behavior which is compatible with vector meson dominance (VMD) and also with pQCD inspired parametrizations [10]:

$$|G_M| = \frac{A(N)}{(q^2)^2 \left[\pi^2 + \ln^2(q^2/\Lambda^2)\right]}, \tag{3}$$

  where $\Lambda = 0.3$ GeV is the QCD scale parameter and $A$ is a free parameter. The best fit for this parametrization, which is the same for proton and neutron, is obtained with $A(p)$= 56.3 GeV$^4$ and $A(n)$= 77.15 GeV$^4$, which reflects the fact that in TL region, neutron FFs are larger than for proton (although few data exist).

- In TL region, proton FFs are twice larger that in SL region.
- Recent data from Babar (radiative return) show that $G_M \neq G_E$, and interesting structures in the $Q^2$ dependence of $G_M$ (still extracted assuming $G_M = G_E$).

In Fig. 1 a large sample of the world data on the form factors for proton (top) and neutron (bottom) electric (left) and magnetic (right) are

reported. For the electric proton FF, the discrepancy among the data measured with the Rosenbluth methods (stars) and the polarization method (solid squares) appears clearly in Fig. 1a. This problem has widely been discussed in the literature and rises fundamental issues. If the trend indicated by polarization measurements is confirmed at higher $Q^2$ by the GEP collaboration, not only the electric and magnetic charge distribution in the nucleus are different and deviate, classically, from an exponential charge distribution, but also the electric FF has a zero and becomes eventually negative.

The data in the TL region are drawn in Fig. 2a, b for the proton and in Fig. 2c, d for the neutron. As no separation has been done for electric and magnetic FFs, the data are extracted under the hypothesis that $|G_{EN}| = |G_{MN}|$. Concerning the neutron, the first and still unique measurement was done at Frascati, by the collaboration FENICE [11]. The models are fitted to the data, assuming that they correspond to $|G_M|$, and the curves in the $|G_E|$ plots should be considered predictions.

Figs. 1 and 2 show that it is possible to find a satisfactory general representation of all nucleon FFs. The parametrization from Ref. [12] (dotted line) is based on a view of the nucleon as composed by an inner core with a small radius (described by a dipole term) surrounded by a meson cloud. The result from [13] (solid line) gives a good overall parametrization, with parameters not far from those found in the original paper for the SL region only.

It is interesting to note that many nucleon models exist and some of them predicted the deviation of $G_{Ep}$ from dipole before the data appeared [12, 15]. However only few of them, in particular VMD parametrizations can describe all the data, electric, magnetic, proton and neutron, in the full kinematical region. Poalrization observables have been derived, and it has been shown that models which fit all existing data, still give very different predictions on polarization observables, and in particular to an angular asymmetry, which can be measured without polarized beam and target [16] (Fig. (3)).

## 3.2 The asymptotic region

The analyticity of FFs allows to apply the Phragmèn-Lindelöf theorem [17] which gives a rigorous prescription for the asymptotic behavior of

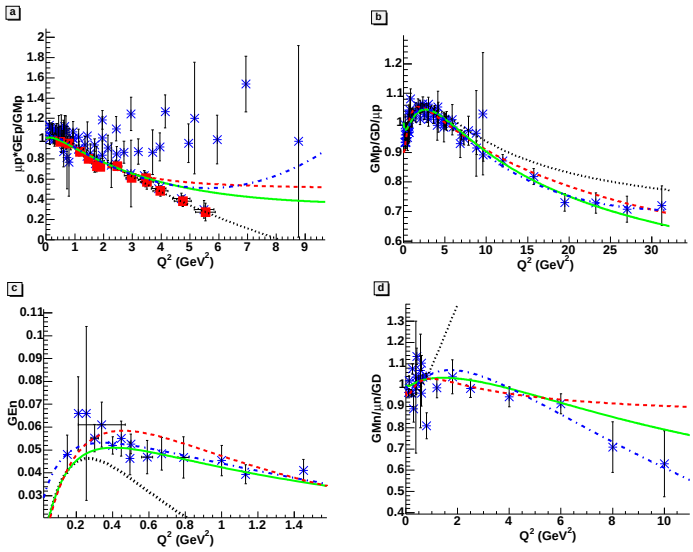


Figure 1: Nucleon Form Factors in SL region: (a) proton electric FF, scaled by $\mu_p G_{Mp}$ (b) proton magnetic FF scaled by $\mu_p G_D$ , (c) neutron electric FF, (d) neutron magnetic FF, scaled by $\mu_n G_D$.See text

analytical functions:

$$\lim_{t\to-\infty} F^{(SL)}(t) = \lim_{t\to\infty} F^{(TL)}(t). \tag{4}$$

This means that, asymptotically, the imaginary part of FFs, in TL region, vanishes: $ImF_i(t) \to 0$, as $t \to \infty$ and that the real part of FFs, in TL region, coincides with the corresponding value in SL region: $ReF_i^{(TL)}(t)[t \to \infty] = F_i^{(SL)}(t)[t \to -\infty]$.

The existing experimental data violate the Phragmèn-Lindelöf theorem, even at $t$ values as large as 18 GeV$^2$ [18]. In order to test the two requirements stated above, the knowledge of the differential cross section for $e^+ + e^- \leftrightarrow p + \bar{p}$ is not sufficient, and polarization phenomena have to be studied also. In this respect, T-odd polarization observables, which are determined by $ImF_1F_2^*$, are especially interesting. The simplest of these observables is the $P_y$ component of the proton polarization in $e^+ + e^- \to p + \bar{p}$ that in general does not vanish, even in collisions of unpolarized leptons [19] with a transversally polarized proton target (or in the collision of transversally polarized antiprotons on an unpolarized proton target) [20]. These observables are especially sensitive to different possible parametrizations

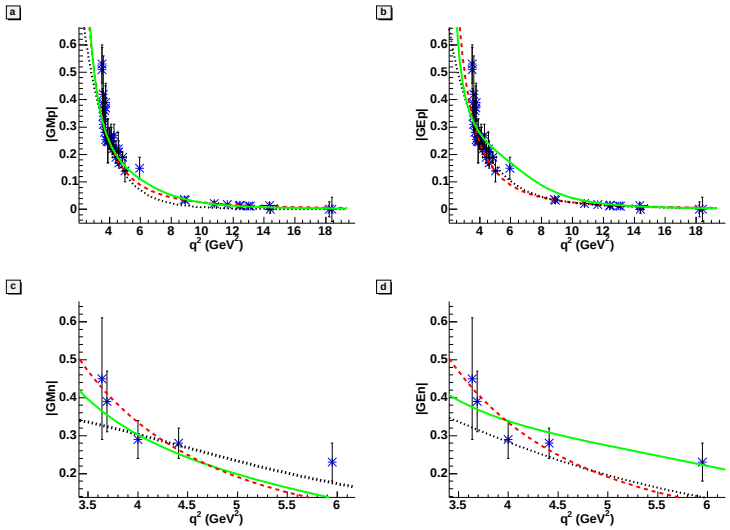


Figure 2: Form Factors in TL region and predictions of the models: pQCD-inspired (dashed line), from Ref. [12] (dotted line), from Ref. [13] (solid line).

of the ratio $R$, suggested by QCD and VDM models. Calculations have been done up to $t \simeq 40$ GeV$^2$ and show that the $P_y$ component remains large in absolute value [21]. For example, QCD inspired parametrizations, which fit reasonably well the data in the SL region, predict $|P_y| \simeq 35\%$ up to $t \simeq 40$ GeV$^2$. Such behavior has to be considered an indication that the corresponding asymptotics are very far.

Note another important property of QCD inspired predictions for nucleon FFs: the corresponding $ImF_i(t)$, $t \geq 4m^2$, $i = 1, 2$ ($m$ is the nucleon mass), either vanish or have a definite sign in the TL region. The previously quoted parametrizations can not apply in the whole TL region: the asymptotic pQCD behavior follows $F_1(t) \simeq t^{-2}$ and $F_2(t) \simeq t^{-3}$ at large $t$, according to the quark counting rules [23]. The superconvergent conditions:

$$\int_{t_0}^{\infty} ImF_i(t)dt = 0, \;\; i = 1, 2 \tag{5}$$

has to be satisfied, where the lower limit corresponds to $t_0 = 4m_\pi^2$, for isovector FFs, and $t_0 = 9m_\pi^2$ for isoscalar FFs, where $m_\pi$ is the pion mass.

This implies that the nonzero QCD-contribution to Eq. (5) has to be compensated by the corresponding non-perturbative contribution of

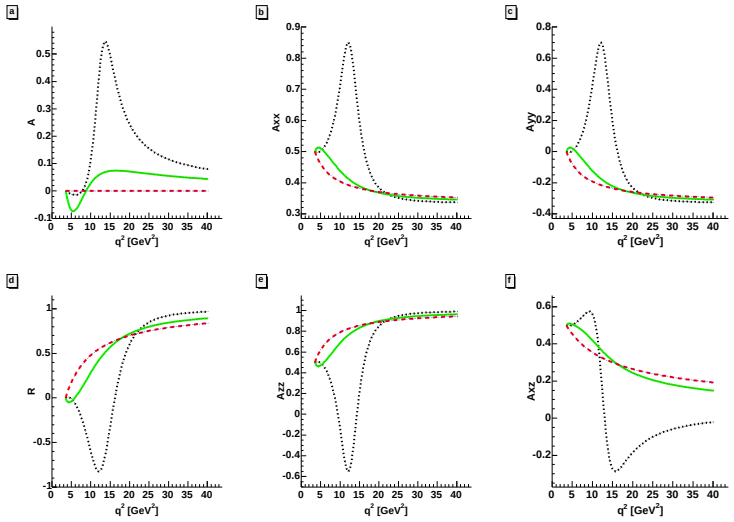


Figure 3: Angular asymmetry and polarization observables, for a fixed value of $\theta = 45^0$. Notations as in Fig. 2.

opposite sign. We can expect that such contribution mainly arises from the special region of $t$: $t_0 \leq t \leq 4m^2$, which is unphysical for the process $e^+ + e^- \leftrightarrow p + \bar{p}$. The contribution from the different vector mesons (with different masses) is expected to be very important here.

Common parametrizations of SL FFs do not satisfy the asymptotic conditions suggested by the Phragmèn-Lindelöf theorem or they do so only for very large values of $Q^2$, well beyond the experimentally accessible range [24]. In particular, the $1/\sqrt{Q^2}$ behavior of this ratio, which reproduces the recent measurements in the SL region, is certainly not compatible with an asymptotic regime, showing that the presently measurable data should be better interpreted in frame of classical nucleon degrees of freedom. The dipole-like formulas for FFs do satisfy the Phragmèn-Lindelöf theorem. But such parametrization has the following evident problems -the threshold condition: $G_{EN}(4m^2) = G_{MN}(4m^2)$ is not satisfied, - the unitarity conditions for all nucleon FFs are strongly violated, as one should have a branching point at $t = 4m_\pi^2$ for isovector FFs and $t = 9m_\pi^2$ for isoscalar FFs, - the prediction in TL region underestimates the experimental data.

# 4 The deuteron

The study of the deuteron structure is especially interesting as it is the simplest nucleus where the nucleon model can be tested. Two aspects are very interesting: - the deuteron can be considered a good neutron target, if its structure is well known, - pQCD gives specific predictions for the FFs and the deuteron structure functions. The measurement of the three deuteron FFs has been done up to $Q^2 = 1.9$ GeV$^2$ [25] and refs. therein. $T_{20}$ data disfavor asymptotic predictions from pQCD and favor a description of deuteron based on relativistic impulse approximation, including different types of corrections. A precise selection of the models is not possible, due to systematics among different sets of data in spite of a precise measurement in the region of the dip [26]. The structure function $A(Q^2)$, related to the forward angle cross section, has been measured up to 6 GeV$^2$. In [27] it was shown that the QCD prediction (5), which can be applied to very large momentum transfer, is working well already for $Q^2 \sim 2$ GeV$^2$, with a plausible value of the parameter $\Lambda \simeq 100$ MeV, in agreement with the values determined by many other possible methods. However, it has been shown [28] that QCD prescriptions for the reduced deuteron FF, and in particular the value of the parameter $\Lambda$ fitted from the data, are extremely sensitive to the choice of the nucleon FFs.

In [29] another interesting prediction, concerning the scaling behavior of the reduced deuteron FF, was done:

$$f_R = \left(1 + \frac{Q^2}{m_0^2}\right) f_D(Q^2) \simeq const, f_D(Q^2) = \frac{\sqrt{A(Q^2)}}{F_N^2(Q^2/4)}, \qquad (6)$$

where $m_0^2 = 0.28$ GeV$^2$ is a parameter related to the $Q^2$-behavior of the pion FF, $F_N$ is the nucleon electromagnetic FF. The same data from [27], if plotted in the representation of the reduced deuteron FFs, should illustrate the $Q^2$-independence of this product. Such result was confirmed by the previous $A(Q^2)$ data [22], in the limit of their accuracy. In Fig. (4) precise data about $A(Q^2)$ [27], are not consistent with the prediction (6) as they show an evident dependence of the product $f_R$ on $Q^2$. This behavior is quite insensitive to different values of the $m_0$ parameter and it holds for different choices of electromagnetic nucleon FF (Fig. 3).

One can conclude that contradictions exist in the interpretation of hadron electromagnetic FFs (nucleon and deuteron) in terms of pQCD, in the intermediate $Q^2$-range (at least up to $Q^2 = 6$ GeV$^2$).

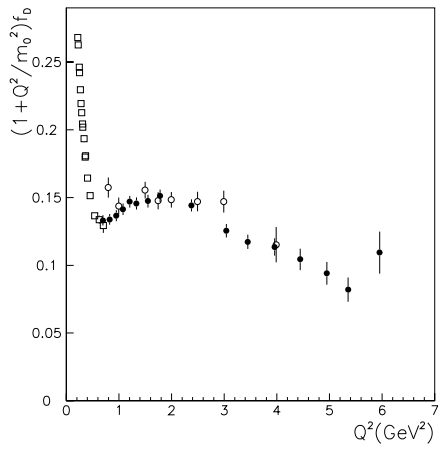


Figure 4: Data set corresponding to the reduced deuteron FFs multiplied by $(1 + Q^2/m_0^2)$. Open circles are from [22], open squares from [30], solid circles from [27].

# 5 Radiative corrections

Electron hadron scattering may give very precise information on the hadron structure as the elctron is considered to be structureless and the reaction mechanism known. However, it is necessary to correct the experimental yield for the photons which are emitted from the incident and the outgoing electron and escape the detection. In case of polarization observables, or, in general of ratios of amplitudes, radiative corrections (RC) are not applied, as their contribution is estimated to be negligible (less than 1%). RC are traditionally applied to the unpolarized differential cross section, following a prescription which includes only leading order contributions as follows [31, 32]:

$$\delta \simeq -\frac{2\alpha}{\pi}\left\{\ln\frac{\Delta E}{E}\left[\ln\left(-\frac{q^2}{m^2}\right)-1\right]+\frac{3}{4}\ln\left(-\frac{q^2}{m^2}\right)+f(\theta)\right\} \qquad (7)$$

where $f(\theta)$ is function only of the scattering angle $\theta$. As noted in the original papers [31, 32], when $\Delta E \to 0$, $\sigma^{meas}$ becomes negatively infinite, whereas physical arguments require that it should vanish. The authors stated already that this problem would be overcome taking into account higher order radiative corrections.

In recent experiments $E$ is large and the experimental resolution is very good (allowing to reduce $\Delta E$). Moreover, multiple photon emission from the initial electron, shifts the momentum transferred to the proton to lower values, increasing the cross section. Therefore $\delta$ becomes sizeable and one can not safely neglect higher order corrections.

A complete calculation of radiative corrections should take into account consistently all different terms which contribute at all orders (including the two photon exchange contribution) and their interference, which becomes extremely complicated. An alternative method for calculating RC is given by the structure function approach, which takes into account higher order of perturbation theory, and, in particular, any number of real and virtual photons, emitted in collinear kinematics [33].

Radiative corrections to elastic $ep$ cross section are usually applied to the data as a global coefficient, which depends on $\epsilon$ and $Q^2$, the relevant variables for the Rosenbluth separation of the FFs. As the radiative corrections become larger, the correlation between the two parameters of the Rosenbluth fit also becomes larger, reaching values near its maximum (in absolute value). Full correlation means that the two parameters are related through a constraint, i.e. it is possible to find a one-parameter description of the data.

The discrepancy amond polarized and unpolaruzed data is not at the level of the observables (the polarization transferred to the scattered proton on one side and the differential cross section on the other side). It has been shown that, calculating $G_{Mp}$ from the measured cross section with the constraint from polarization measurements, leads to a renormalization of $G_{Mp}$ of the order of 2-3% only, with respect to the Rosenbluth data [34], well inside the error bars. The data are not consistent if one refers to the slope of the $\epsilon$ dependence of the reduced cross section, which is directly related to $G_{Ep}$, as shown in particular by the recent precise data [35]

It was shown [36], in a model independent way, that the presence of two-photon exchange destroys the linearity of the Rosenbluth fit, inducing a specific dependence of the differential cross section on the variable $\epsilon$, which is especially large for $\epsilon \to 1$. Such linearity has been confirmed from all the existing data at the level of 1% [37].

In presence of $2\gamma$ exchange, Eq. (1) can be rewritten in the following general form:

$$\sigma_{red}(Q^2, \epsilon) = \epsilon G_E^2(Q^2) + \tau G_M^2(Q^2) + \alpha F(Q^2, x), \tag{8}$$

where $\alpha = e^2/(4\pi)$, and $F(Q^2, x)$ is a real function (of both independent variables $Q^2$ and $\epsilon$), describing the effects of the $1\gamma \bigotimes 2\gamma$ interference which can be parametrized as:

$$F(Q^2, \epsilon) \to \epsilon x f^{(T)}(Q^2),\ x = \sqrt{\frac{1+\epsilon}{1-\epsilon}}. \tag{9}$$

C-invariance and the crossing symmetry of hadron electromagnetic interaction, result in the following symmetry properties $F(Q^2, x) = -F(Q^2, -x)$ [36].

This means that the $1\gamma \bigotimes 2\gamma$ contribution $F(Q^2, x)$ has an essential non linear $\epsilon$ dependence, at any $Q^2$. It is important to stress that Eq. (9) is a simple expression which contains the necessary symmetry properties of the $1\gamma \bigotimes 2\gamma$ interference, through a specific (and non linear) $\epsilon$ dependence.

For the $Q^2$ dependence of $f^{(T,A)}$ we take:

$$f^{(T,A)}(Q^2) = C/\{[(1 + Q^2[\mathrm{GeV}]^{\ 2}/0.71)^2(1 + Q^2[\mathrm{GeV}]^2/m^2_{T,A})^2\}, \tag{10}$$

where $C$ is a fitting parameter, $m_{T,A} \simeq 1.5$ GeV$^2$ is the mass of a tensor or an axial meson with positive C-parity.

Taking into account the $\alpha$ term which is included in Eq. (8), the deviation of linearity, which is quantified by the parameter $C$ is smaller than 1%. In average, the dominating term is the magnetic term with a contribution at the level of $(95.9 \pm 0.3)\%$. The electric term contributes for $(3.8 \pm 0.3)\%$ and the average for the two photon term is $(0.05 \pm 0.05)\%$ in the considered sets of data.

In Ref. [38] it was shown that the $G_E(p)/G_M(p)$ problem can be solved by taking into account initial state emission, in the structure function (SF) [33] approach and that the $2\gamma$ exchange mechanism is irrelevant for the solution of this problem. The cross section can be expressed in terms of SF of the initial electron and of the fragmentation function of the scattered electron energy fraction. The dependence of the differential cross section on the angle and the energy fraction of the scattered electron $y = 1/\rho$ ($\rho$ is the recoil factor $\rho = 1 + (E/M)(1 - \cos\theta)$ ) can be written as:

$$\frac{d\sigma}{d\Omega dy} = \int_{z_0}^{1} \frac{dz\rho_z}{z} D(z) D\left(\frac{y\rho_z}{z}\right) \frac{\Phi_0(z)}{|1 - \Pi(Q_z^2)|^2} \left(1 + \frac{\alpha}{\pi} K\right). \tag{11}$$

The term $K = K_e + K_p + K_{box}$ includes all the non-leading terms, as two photon exchange and soft photon emission and it is the sum of three contributions. $K_e$ is related to non leading contributions arising from the pure

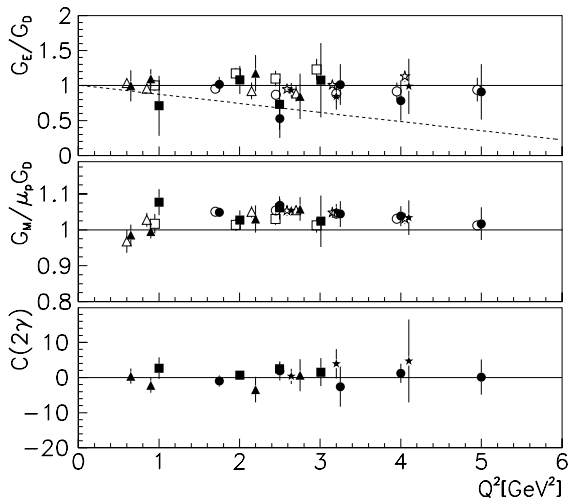


Figure 5: From top to bottom: $G_{Ep}/G_D$, $G_{Mp}/\mu_p G_D$, and two-photon contribution, $C$ (Eq. (10)). The results including $2\gamma$ contribution are shown as solid symbols. The abscissa of the published data (open symbols) is shifted by -100 KeV, for clarity. The expectation from polarized data is shown as a dashed line.

electron block, $K_p$ concerns the emission of virtual and soft photons by the proton which is not associated with large logarithm, and $K_{box}$ represents the interference between the two virtual photon exchange amplitude and the Born amplitude and the relevant part of the soft photon emission. This effect is not enhanced by large logarithm (characteristic of SF) and can be considered among the non-leading contributions.

The numerical results strongly depend on the experimental conditions, in particular on the inelasticity cut of the scattered electron energy spectrum (here $c = 0.97$). In Fig. 6 the results are shown as a function of $\epsilon$, for $Q^2 = 1$, 3, and 5 GeV$^2$, from top to bottom. The calculation based on the structure function method is shown as dashed lines. The full calculation, including the two-photon exchange contribution is shown as dash-dotted lines. For comparison the results corresponding to the Born reduced cross section are shown as solid lines.

One can see that the main effect of the present calculation is to modify

and to lower the slope of the reduced cross section. This effect gets larger with $Q^2$. Non-linearity effects are small and induced by the $y$ integration. Including two-photon exchange modifies very little the results, in the kinematical range presented here.

The relative effect of the corrections is of the order of the corrections to the unpolarized cross section and it is very similar for the longitudinal and transversal polarized components. Therefore the ratio of the polarizations is very little affected by radiative corrections.

One can tentatively extract the FFs ratio, after correcting the measured unpolarized cross section by the ratio of the Born to the SF results. It is an average correction, which is not applied event by event, but it takes into account the main feature of the SF calculation, i.e., the lowering of the slope of the unpolarized cross section as a function of $\epsilon$. We neglect the correction from the two photon exchange, as it is negligible when compared to the high order corrections. The $Q^2$-dependence of the ratio $R = \mu G_E/G_M$ is plotted in Fig. 7, for the sets of data for which a detailed information on RC was published . Open symbols refer to the published data, the corresponding solid symbols represent the corrected data. At low $Q^2$, (triangles) RC are small, and high order corrections affect very little the results. Data from the polarization method are shown as stars, fitted by a linear function.

The present results suggest that an appropriate treatment of radiative corrections constitutes the solution of the discrepancy between form factors extracted by the Rosenbluth or by the recoil polarization method.

# 6 Conclusion

In these lectures we have summarized experimental results and given a critical view on some aspects of nucleon and deuteron structure. We have shown that this domain is very rich and large perspectives are opened at present and future machines, as JLab, VEPP, BES, FAIR. In particular, new information is expected in the time-like region.

Many of the ideas presented in these lectures were inspired by Prof. M. P. Rekalo. The work presented here has been possible in frame of fruitful collaborations. In particular, I acknowledge the members of the ALPOM and GEP collaborations, and the co-authors of several papers quoted here: G.I. Gakh, V. Bytyev, Y. Bystriskyi and E.A. Kuraev also for careful reading of the manuscript.

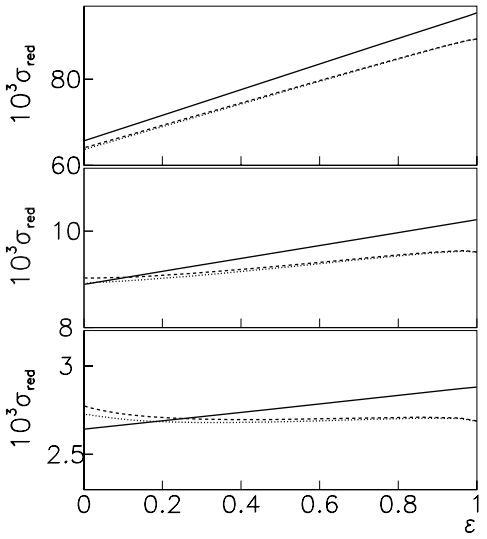


Figure 6: The $\epsilon$-dependence of the elastic differential cross section, for $Q^2$ = 1, 3, and 5 GeV$^2$, from top to bottom: Born cross section (solid line), Drell-Yan cross section (dashed line), full calculation (dash-dotted line) (including Born, SF and K-factor contributions).

# References


[1] M. N. Rosenbluth, Phys. Rev. **79**, 615 (1950).

[2] A. Akhiezer and M. P. Rekalo, Dokl. Akad. Nauk USSR, **180**, 1081 (1968); Sov. J. Part. Nucl. **4**, 277 (1974).

[3] V. Punjabi *et al.*, Phys. Rev. C 71 (2005) 055202 [Erratum-ibid. C **71** (2005) 069902] and refs. therein.

[4] E. Tomasi-Gustafsson *et al.*, Nucl. Instrum. Meth. A **420**, 90 (1999).

[5] I. Sitnik *et al.*, Nucl. Phys. A **663** (2000) 443; E. Tomasi-Gustafsson, I. M. Sitnik, C. F. Perdrisat and M. P. Rekalo, Nucl. Instrum. Meth. A **402**, 361 (1998).

[6] S. Kox *et al.*,Nucl. Instrum. Meth. A **346**, 527 (1994).

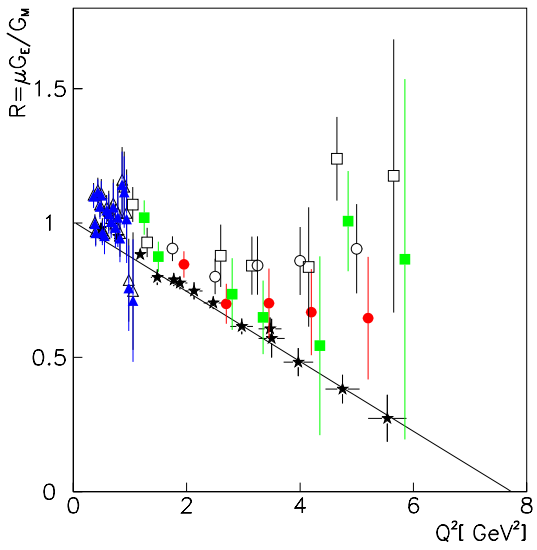


Figure 7: The $Q^2$-dependence of the FF ratio. Data from Rosenbluth method before (open symbols) and after (solid symbols) correction. Data from polarization method [3] are also shown (stars). The line is a fit to the polarization data.


[7] D. Abbott *et al.* [JLAB t(20) Collaboration], Phys. Rev. Lett. **84**, 5053 (2000).

[8] I. Pomeranchuk, Dokl. Akad. Nauk CCCR, **78**, 249 (1951).

[9] I. M. Sitnik, Nucl. Instrum. Meth. A **527**, 278 (2004).

[10] D. V. Shirkov and I. L. Solovtsov, Phys. Rev. Lett. **79**, 1209 (1997).

[11] A. Antonelli *et al.*, Nucl. Phys. B **517**, 3 (1998).

[12] F. Iachello, A. D. Jackson and A. Lande, Phys. Lett. B **43**, 191 (1973).

[13] E. L. Lomon, Phys. Rev. C **66**, 045501 (2002).

[14] G. Hohler, E. Pietarinen, I. Sabba Stefanescu, F. Borkowski, G. G. Simon, V. H. Walther and R. D. Wendling, Nucl. Phys. B **114**, 505 (1976);

[15] G. Holzwarth, Z. Phys. A **356**, 339 (1996).

[16] E. Tomasi-Gustafsson, F. Lacroix, C. Duterte and G. I. Gakh, Eur. Phys. J. A **24**, 419 (2005).

[17] E. C. Titchmarsh, *Theory of functions*, Oxford University Press, London, 1939.

[18] E. Tomasi-Gustafsson and M. P. Rekalo, Phys. Lett. B **504**, 291 (2001) and refs herein.

[19] A. Z. Dubnickova, S. Dubnicka and M. P. Rekalo, Nuovo Cim. A **109**, 241 (1996).

[20] S. M. Bilenkii, C. Giunti and V. Wataghin, Z. Phys. **C59**, 475 (1993).

[21] S. J. Brodsky, C. E. Carlson, J. R. Hiller and D. S. Hwang, Phys. Rev. D **69**, 054022 (2004).

[22] R. G. Arnold *et al.*, Phys. Rev. Lett. **57**, 174 (1986).

[23] V. Matveev *et al.*, Nuovo Cimento Lett. **7**, 719 (1973).

[24] E. Tomasi-Gustafsson and G. I. Gakh, Eur. Phys. J. A **26**, 285 (2005)

[25] D. Abbott *et al.* [JLAB t(20) Collaboration], Phys. Rev. Lett. **84**, 5053 (2000).

[26] D. M. Nikolenko *et al.*, Phys. Rev. Lett. **90**, 072501 (2003).

[27] L. C. Alexa *et al.*, Phys. Rev. Lett. **82**, 1374 (1999).

[28] E. Tomasi-Gustafsson and G. I. Gakh, Eur. Phys. J. A **26**, 285 (2005).

[29] S. J. Brodsky and B. T. Chertok, Phys. Rev. D **14**, 3003 (1976); Phys. Rev. Lett. **37**, 269 (1976); S. J. Brodsky, C. R. Ji and G. P. Lepage, Phys. Rev. Lett. **51**, 83 (1983).

[30] S. Platchkov *et al.*, Nucl. Phys **A510**, 740 (1990).

[31] L. W. Mo and Y. S. Tsai, Rev. Mod. Phys. **41**, 205 (1969).

[32] J. S. Schwinger, Phys. Rev. **76**, 790(1949).

[33] E. A. Kuraev and V. S. Fadin, Sov. J. Nucl. Phys. **41**, 466 (1985) [Yad. Fiz. **41**, 733 (1985)];

[34] E. J. Brash, A. Kozlov, S. Li and G. M. Huber, Phys. Rev. C **65** 051001(R) (2002).

[35] I. A. Qattan *et al.*, Phys. Rev. Lett. **94**, 142301 (2005).

[36] M. P. Rekalo, E. Tomasi-Gustafsson and D. Prout, Phys. Rev. C **60**, 042202R (1999); M. P. Rekalo and E. Tomasi-Gustafsson, Eur. Phys. J. A. **22**, 331 (2004).

[37] E. Tomasi-Gustafsson and G. I. Gakh, Phys. Rev. C **72**, 015209 (2005).

[38] Yu. M. Bystritskiy, E. A. Kuraev and E. Tomasi-Gustafsson, Phys. Rev. C **75**, 015207 (2007).